Int. J. Solids Structures Vol. 22, No. 12, pp. 1557–1570, 1986
Printed in Great Britain.

0020-7683/86 $3.00 + .00
Pergamon Journals Ltd.

THE FINITE DEFORMATION OF INTERNALLY PRESSURIZED HOLLOW CYLINDERS AND SPHERES FOR A CLASS OF COMPRESSIBLE ELASTIC MATERIALS

D.-T. CHUNG, C. O. HORGAN and R. ABEYARATNE†
College of Engineering, Michigan State University, East Lansing, MI 48824-1226, U.S.A.

(*Received* 27 *June* 1985; *in revised form* 14 *November* 1985)

Abstract—The finite elastic deformation of hollow circular cylinders and spheres under applied uniform internal pressure is studied and conditions for the initiation of a localized shear bifurcation are obtained. The location of this bifurcation relative to the pressure maximum is investigated. It is shown that when the ratio of the outer undeformed radius to the inner undeformed radius is larger than a critical value, the shear bifurcation occurs before the pressure maximum is attained, while when this ratio is smaller than the critical value, the converse is true. The analysis is carried out for a particular compressible elastic foam rubber material (the Blatz–Ko material). The results are obtained in closed analytic form.

1. INTRODUCTION

Recently Abeyaratne and Horgan[1] obtained an exact solution to a problem describing finite plane strain deformation of an infinite medium, composed of a certain compressible nonlinearly elastic material, the so-called Blatz–Ko material. The problem considered in [1] concerned an infinite medium with a circular cylindrical cavity under pressure loading conditions. In this paper we show that the solution technique of [1] may be applied also to the case of pressurized hollow cylinders and spheres with finite radii, and we carry out a detailed investigation of the solution to these basic problems of nonlinear elasticity.

The material considered in this study is a particular homogeneous, isotropic, compressible elastic material, namely the Blatz–Ko material. The pressurized cylinder and sphere problems in finite elasticity for incompressible materials have been considered previously by many authors (see e.g. [2, 3]) and are simpler, since the incompressibility constraint immediately yields an explicit expression for the (axially symmetric) deformation field. Such simplification does not occur for compressible materials.‡

The "Blatz–Ko material" is a mathematical model characterizing the constitutive behavior of a certain foam rubber-like material and was proposed by Blatz and Ko[7] on the basis of experiments carried out by them. An extensive discussion of its properties may be found in [7] and also in the paper of Knowles and Sternberg[8]. One interesting feature of the Blatz–Ko material is that the system of partial differential (displacement) equations governing the equilibrium of a body composed of such a material may cease to be elliptic at sufficiently severe strain levels[8]. In the present work, we are interested in examining the implications of this for the pressurized cylinder and sphere problems.

In the next section, the problem of a hollow circular cylinder composed of the Blatz–Ko material subject to internal pressure is formulated. In Sections 3 and 4, the solution to the resulting boundary value problem is obtained and features of the solution are discussed. In particular, it is found that as the applied pressure p is increased from zero, the deformed radius increases until p reaches a maximum value. Subsequently, p decreases even though the deformed radius still increases (see Figs 1 and 2). Such non-monotone pressure vs radius relationships are well known in finite elasticity, particularly for incompressible

† Present address: Department of Mechanical Engineering, Massachusetts Institute of Technology, Cambridge, MA 02139, U.S.A.

‡ The pressurized sphere and cylinder problems for a class of (hypothetical) compressible materials, namely harmonic materials, have been investigated recently[4, 5]. See also [3, Chapter 5; 6].

materials.† In Section 4, we also examine the loss of ellipticity of the governing displacement equations of equilibrium at the deformation at hand. The value of the applied pressure (and the corresponding deformed inner radius) at which the cylinder first loses ellipticity is obtained. It is shown that when the ratio of the outer undeformed radius to the inner undeformed radius is larger than a critical value, loss of ellipticity occurs before the pressure maximum is attained while when this ratio is smaller than this critical value, the converse is true.

Analogous results for the corresponding problem for a hollow sphere are obtained in Section 5.

2. THE PRESSURIZED HOLLOW CYLINDER; FORMULATION OF BOUNDARY-VALUE PROBLEM

Let the open region $D_0 = \{(r, \theta) \mid a < r < b, 0 < \theta < 2\pi\}$ denote the cross-section of a right circular cylinder with inner radius a, and outer radius b, in its undeformed configuration. The cylinder is subjected to an internal pressure of magnitude p. The resulting deformation is a one-to-one mapping which takes the point with polar coordinates (r, θ) in the undeformed region D_0 to the point (R, Θ) in the deformed region D. We assume that the deformation is an axisymmetric plane strain one so that

$$R = R(r) > 0, \quad \Theta = \theta \text{ on } D_0, \tag{2.1}$$

where the positive function $R(r)$ is to be determined. Unless explicitly stated otherwise $R(r)$ is assumed to be twice continuously differentiable on $a < r < b$.

The polar components of the deformation gradient tensor $\mathbf{F}$ associated with (2.1) are given by

$$\mathbf{F} = \text{diag}\,(\dot{R}(r), R(r)/r), \tag{2.2}$$

where the dot denotes differentiation with respect to the argument. The Jacobian determinant $J = \det \mathbf{F}$ is required to be positive and hence one has

$$\dot{R}(r) > 0 \quad \text{for } a < r < b. \tag{2.3}$$

The principal stretches associated with the radial deformation (2.1) are

$$\lambda_r = \dot{R}(r), \quad \lambda_\theta = R(r)/r. \tag{2.4}$$

The right Cauchy–Green deformation tensor is defined as $\mathbf{C} = \mathbf{F}^T\mathbf{F}$ and its fundamental scalar invariants can be taken as

$$I = tr\mathbf{C}, \quad J = (\det \mathbf{C})^{1/2} \tag{2.5}$$

so that in the present problem

$$I = \dot{R}^2 + (R/r)^2, \quad J = R\dot{R}/r. \tag{2.6}$$

Next we turn to the constitutive relation and suppose that the cylinder is composed of a Blatz–Ko material[7]. An extensive discussion of the stress response of this material to various states of deformation may be found in [8]. This compressible, isotropic, elastic material is characterized, in plane strain, by the elastic potential

$$W(I, J) = \mu/2(I/J^2 + 2J - 4), \quad \mu > 0, \tag{2.7}$$

† An extensive study of this phenomenon for incompressible materials has been carried out recently by Carroll[9]. It is of interest to note that this behavior does not occur in the cylindrical inflation of Mooney–Rivlin or neo-Hookean (incompressible) materials whereas it does for spherical inflation of such materials[9].

representing the strain energy per unit undeformed volume. Here μ denotes the shear modulus of the material at infinitesimal deformations. The true stress tensor τ associated with a plane deformation is given by

$$\tau = (2J^{-1}\partial W/\partial I)\mathbf{F}\mathbf{F}^T + (\partial W/\partial J)\mathbf{1}. \tag{2.8}$$

On substituting from (2.7) and (2.6) into (2.8) one finds that

$$\tau_{RR}(r) = \mu\left(1 - \frac{r}{R(r)\dot{R}^3(r)}\right), \tag{2.9a}$$

$$\tau_{\Theta\Theta}(r) = \mu\left(1 - \frac{r^3}{R^3(r)\dot{R}(r)}\right), \tag{2.9b}$$

$$\tau_{R\Theta} = \tau_{\Theta R} = 0, \quad a < r < b. \tag{2.9c}$$

In the absence of body forces, the equilibrium equations $\operatorname{div}\tau = \mathbf{0}$ in the present case reduce to the single equation:

$$\frac{\mathrm{d}}{\mathrm{d}r}\tau_{RR} + \frac{\dot{R}}{R}(\tau_{RR} - \tau_{\Theta\Theta}) = 0, \quad \text{for } a < r < b. \tag{2.10}$$

This, together with (2.9), yields the following nonlinear second-order ordinary differential equation for $R(r)$:

$$3rR^3\ddot{R} - R^3\dot{R} + r^3\dot{R}^4 = 0 \quad \text{for } a < r < b. \tag{2.11}$$

The prescribed boundary conditions are

$$\tau_{RR} = -p \quad \text{at } r = a, \qquad \tau_{RR} = 0 \quad \text{at } r = b, \tag{2.12}$$

which, on using (2.9), can be written as

$$R(a)\dot{R}^3(a) = a(1 + p/\mu)^{-1}, \tag{2.13a}$$

$$R(b)\dot{R}^3(b) = b. \tag{2.13b}$$

In the next section we derive an exact solution to the boundary-value problem (2.11), (2.13).

3. SOLUTION OF BOUNDARY-VALUE PROBLEM

3.1. *Solution*

It has been shown recently in [1] that the second-order nonlinear ordinary differential equation (2.11) may be reduced to a first-order equation on making the substitution

$$t(r) = \frac{r\dot{R}(r)}{R(r)} (= \lambda_r/\lambda_\theta) > 0. \tag{3.1}$$

Equation (2.11) then yields

$$3r\dot{t} - t(1-t)(t^2 + t + 4) = 0 \quad \text{for } a < r < b, \tag{3.2}$$

where $\dot{t} = \mathrm{d}t/\mathrm{d}r$. It can be shown that there is no loss of generality in assuming that $t(r)$ is less than unity† for $a < r < b$. Thus it then follows from (3.2) that t increases monotonically

† The arguments given in [1] to justify this assumption carry over, with obvious modification, to the present problem. Notice that since the applied load is that of internal pressure only, one would expect $\lambda_r < 1$, $\lambda_\theta > 1$ and so one anticipates that t is indeed less than unity.

with increasing r and so we have

$$0 < t < 1, \quad dt/dr > 0 \quad \text{for } a < r < b. \tag{3.3}$$

Upon integrating (3.2), one finds that

$$r^8 = \frac{Ct^6 h(t)}{(1-t)^4(t^2+t+4)}, \tag{3.4}$$

where $C > 0$ is a constant of integration and we have set

$$h(t) = \exp\left\{\frac{6}{\sqrt{15}}\tan^{-1}\left(\frac{2t+1}{\sqrt{15}}\right)\right\} > 0. \tag{3.5}$$

On the other hand (3.1) and (3.2) also give

$$\frac{1}{R}\frac{dR}{dt} = \frac{3}{(1-t)(t^2+t+4)} > 0, \tag{3.6}$$

which yields

$$R^4 = \frac{D(t^2+t+4)h(t)}{(1-t)^2}. \tag{3.7}$$

Again, $D > 0$ is a constant of integration. Observe from (3.3), (3.6) that the undeformed and deformed radial coordinates (r, R) vary monotonically with t. Equations (3.4), (3.5), (3.7) provide a parametric solution to the differential equation (2.11). The range of the parameter t is

$$t_a < t < t_b, \tag{3.8}$$

where $t_a > 0$ is the value of t corresponding to $r = a$ and is to be determined from (3.4) and $t_b < 1$ is determined in an analogous fashion. The components of true stress τ_{RR}, $\tau_{\theta\theta}$ may also be expressed in terms of t on using (2.9), (3.1), (3.4) and (3.5). This leads to

$$\tau_{RR} = \mu\left[1 - \frac{\sqrt{C/D^2}}{\sqrt{h(t)}(t^2+t+4)^{3/2}}\right], \tag{3.9}$$

$$\tau_{\theta\theta} = \mu\left[1 - \frac{t^2\sqrt{C/D^2}}{\sqrt{h(t)}(t^2+t+4)^{3/2}}\right], \quad t_a < t < t_b. \tag{3.10}$$

From the definition of t_a, t_b, it follows from (3.4) that

$$a^8 = \frac{Ct_a^6 h(t_a)}{(t_a^2+t_a+4)(1-t_a)^4}, \tag{3.11}$$

$$b^8 = \frac{Ct_b^6 h(t_b)}{(t_b^2+t_b+4)(1-t_b)^4}. \tag{3.12}$$

Finally the boundary conditions (2.12), in view of (3.9), may be written as

$$-p = \mu\left\{1 - \frac{\sqrt{C/D^2}}{\sqrt{h(t_a)}(t_a^2+t_a+4)^{3/2}}\right\}, \tag{3.13}$$

$$0 = \mu\left\{1 - \frac{\sqrt{C/D^2}}{\sqrt{h(t_b)(t_b^2+t_b+4)^{3/2}}}\right\}. \tag{3.14}$$

Equations (3.11)–(3.14) consist of four equations for the four unknowns t_a, t_b, C and D. In the following sub-section we discuss the existence of solutions to these equations.

3.2. *Discussion*

We eliminate the integration constant C between eqns (3.11) and (3.12) and obtain

$$b^8 g(t_b) = a^8 g(t_a), \tag{3.15}$$

where $g(t)$ is given by

$$g(t) = \frac{(t^2+t+4)(1-t)^4}{t^6 h(t)}, \quad 0 < t < 1. \tag{3.16}$$

Also from (3.13) and (3.14), eliminating the constants C/D^2, one has

$$\left(1+\frac{p}{\mu}\right)^2 = \frac{h(t_b)(t_b^2+t_b+4)^3}{h(t_a)(t_a^2+t_a+4)^3}. \tag{3.17}$$

Thus we now have two eqns (3.15) and (3.17) for the two unknowns t_a and t_b. The function $g(t)$ in eqn (3.16) tends to infinity as $t \to 0+$, decreases monotonically as t increases and has the value zero when $t = 1$. Thus for a given ratio of outer undeformed radius b to inner undeformed radius a, one can always express t_a in terms of t_b and vice versa. We may write

$$t_b = f(t_a, \alpha) \tag{3.18}$$

where $\alpha = b/a$ and f is an implicit function. Thus, for a given applied pressure p, if (3.17) with t_b expressed as in (3.18), can be solved for a number t_a such that $0 < t_a < 1$, then (3.18) provides a number t_b and (3.11)–(3.14) is the desired solution.

In order to verify that (3.17) can indeed be solved for an appropriate value of t_a, we consider the auxiliary function $Q(t_a)$ defined by

$$Q(t_a) \equiv \frac{h(f(t_a))\{f^2(t_a)+f(t_a)+4\}^3}{h(t_a)(t_a^2+t_a+4)^3}, \quad 0 < t_a < 1, \tag{3.19}$$

which appears on the right-hand side of (3.17), when (3.18) is taken into account. For convenience here, we have written $f(t_a) \equiv f(t_a, \alpha)$. One can readily show that

$$\begin{aligned} &\lim_{t_a \to 0+} Q(t_a) = 1, \\ &\lim_{t_a \to 0+} \frac{dQ(t_a)}{dt_a} > 0, \\ &\lim_{t_a \to 1-} Q(t_a) = 1, \\ &\lim_{t_a \to 1-} \frac{dQ(t_a)}{dt_a} < 0. \end{aligned} \tag{3.20}$$

It follows that for $0 < t_a < 1$, there exists a maximum value for Q, with the corresponding value of p given by (3.17) as $p = p_m$. Thus, if $0 < p < p_m$, there exist at least two solutions for t_a. It is shown in [10] that Q has only one local maximum and so exactly two solutions for t_a exist.

Finally, we observe that the deformed inner radius $R(a)$, given by (3.7) with $t = t_a$,

may be written as

$$\frac{R(a)}{a} = t_a^{-3/4}(1+p/\mu)^{-1/4}, \tag{3.21}$$

on using (3.11) and (3.13).

4. RESULTS AND DISCUSSION

We now examine some features of the results derived in the previous section and consider some illustrative examples.

4.1. *Thin shells*

When the radius ratio $\alpha = b/a$ is very near to unity, it is not difficult to express the relation (3.18) between t_a and t_b explicitly. Let

$$\alpha = 1+\varepsilon, \quad \varepsilon = (b-a)/a(\ll 1), \tag{4.1}$$

and assume

$$t_b = t_a + \varepsilon A(t_a), \tag{4.2}$$

where $A(t)$ is an, as yet, unknown function. Substituting (4.1), (4.2) into eqn (3.15) and neglecting second-order terms in ε yields $A(t) = 1/3(t^2+t+4)(1-t)t$ and so (4.2) then reads

$$t_b = t_a + (\varepsilon/3)(t_a^2+t_a+4)(1-t_a)t_a, \quad 0 < t_a < 1. \tag{4.3}$$

Upon substituting from (4.3) into eqn (3.17), one obtains an explicit relation between t_a and the prescribed pressure, which is given, to leading order, by

$$p/\mu = \varepsilon(t_a - t_a^3), \quad \text{for } 0 < t_a < 1. \tag{4.4}$$

It is clear from (4.4) that p has only one maximum. The deformed cavity radius $R(a)$, is given by (3.21). In the present case, where p is given by (4.4), eqn (3.21) yields, to leading order,

$$\frac{R(a)}{a} = t_a^{-3/4}, \tag{4.5}$$

where the value of t_a corresponding to a prescribed pressure p is found from (4.4). A graph of the ratio of the deformed radius to undeformed radius vs pressure, according to (4.4), (4.5), is shown in Fig. 1. As the pressure p is increased from zero, the deformed radius increases until p reaches a maximum value of $0.385\mu\varepsilon$, where $R(a) = 1.510a$. Subsequently p decreases even though the radius still increases. This phenomenon is well known in finite elasticity, especially for incompressible materials (see e.g. Ogden[3], pp. 283–287 for the spherical thin shell and the comprehensive recent study by Carroll[9]).

4.2. *Thick cylinder*

For a thick-walled cylinder, the relation between t_a and t_b is implicit and thus computational work is necessary, in general to analyze the behavior of pressure vs radius. As observed in Section 3, it is shown analytically in [10] that p has only one maximum point. A graph of the ratio of the deformed radius to undeformed radius vs pressure, obtained from solving (3.15), (3.17) numerically and using (3.21), is shown in Fig. 2, for different values of the radius ratio $\alpha = b/a$. As is shown in Fig. 2, as the thickness of the cylinder increases, the value of the maximum pressure increases and it occurs at increasingly larger values of $R(a)/a$, as might be expected.

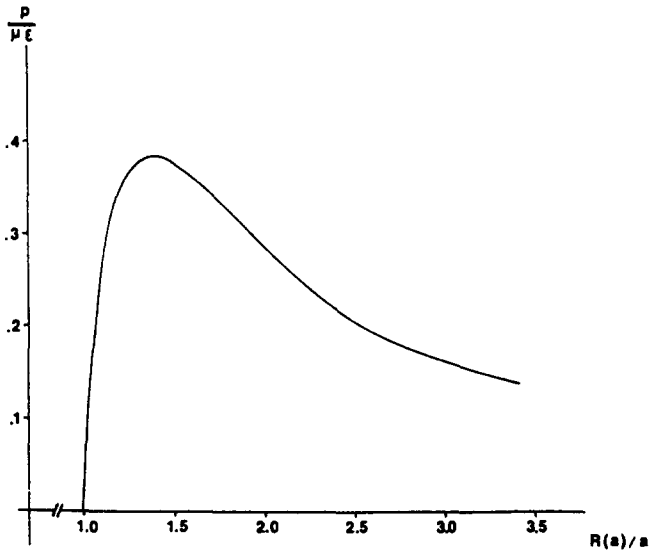

Fig. 1. Applied pressure vs ratio of deformed to undeformed radius for a thin cylindrical shell.

The bottom curve in Fig. 2, corresponding to $\alpha = 1.05$, is seen to confirm the thin shell results discussed in sub-section 4.1. On the other hand, as $\alpha \to \infty$ (i.e. a cavity in an infinite medium), the pressure maximum is reached asymptotically as the deformed radius tends to infinity, and has the value $p_m = 1.51677\mu$. Thus we recover the result of [1] for this case.

4.3. *Linearization*

In the particular case when the applied pressure is small ($p/\mu \ll 1$), (3.19) and (3.21) show that $t_a \simeq 1$, $t_b \simeq 1$ and so $t(r) \simeq 1$ throughout the body. Let

$$t_a = 1-\delta_a, \quad t_b = 1-\delta_b, \quad t(r) = 1-\delta(r), \tag{4.6}$$

where the small parameters $\delta(r)$, δ_a, δ_b are unknown. Substituting (4.6) into (3.9), (3.10), (3.13), (3.14) yields, to leading order,

$$\tau_{\theta\theta} = \mu(\delta_b+\delta), \tag{4.7}$$

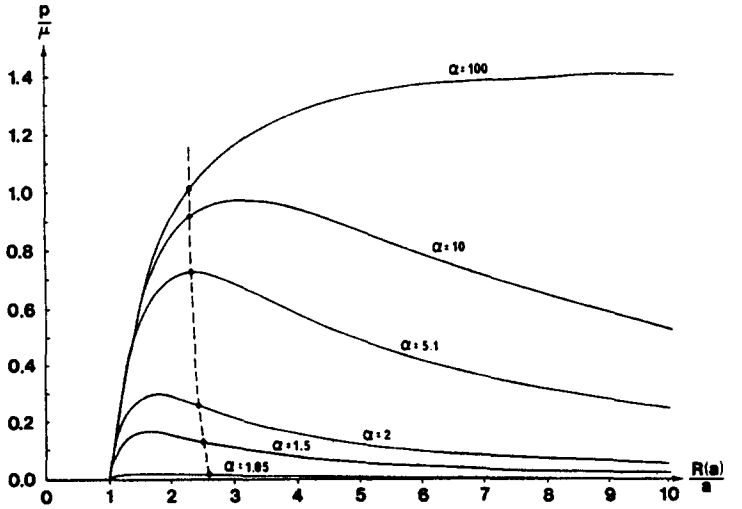

Fig. 2. Applied pressure vs ratio of deformed to undeformed radius for hollow cylinders for different radius ratios $\alpha = b/a$. The dotted curve connects the points $(p_e/\mu, R(a)/a)$, where p_e denotes the pressure at which ellipticity is lost.

$$\tau_{RR} = \mu(\delta_b - \delta), \tag{4.8}$$

$$p/\mu = \delta_a - \delta_b. \tag{4.9}$$

Also from (3.4), (3.11), using (4.6), one obtains

$$\delta(r) = \left(\frac{a^2}{r^2}\right)\delta_a. \tag{4.10}$$

Finally the relation between δ_a and δ_b may be obtained upon substituting (4.6) into (3.15). This leads to

$$\delta_b = \delta_a \alpha^{-2}, \quad (\alpha = b/a). \tag{4.11}$$

The resulting linearized stress fields given by (4.7)–(4.11) yield the well-known results of the infinitesimal theory of elasticity (see e.g. Timoshenko and Goodier[11], p. 71):

$$\tau_{\theta\theta} = \frac{pa^2}{b^2 - a^2}\left(1 + \frac{b^2}{r^2}\right), \tag{4.12}$$

and

$$\tau_{RR} = \frac{pa^2}{b^2 - a^2}\left(1 - \frac{b^2}{r^2}\right). \tag{4.13}$$

4.4. *Loss of ellipticity*

It is well known that the displacement equations of equilibrium in finite elastostatics may lose ellipticity at sufficiently severe deformations. In particular, for the Blatz–Ko material, necessary and sufficient conditions (in terms of the principal stretches) for ellipticity have been obtained by Knowles and Sternberg[8]. In this sub-section, we examine the implications of these results for the pressurized cylinder problem at hand.

From eqn (4.8) of [8], it follows that ellipticity holds for the Blatz–Ko material (2.7) at the axisymmetric solution (2.1) if and only if the principal stretches λ_r, λ_θ introduced in (2.4) are such that

$$2 - \sqrt{3} < t < 2 + \sqrt{3}, \quad (t = \lambda_r/\lambda_\theta). \tag{4.14}$$

Since in the present problem we have $0 < t < 1$, it follows that the right hand inequality here always holds. On the other hand, it is clear that ellipticity will be lost whenever the left inequality is violated.

In view of the monotonic increasing character of t as r increases [see (3.3)], and recalling that $0 < t_a < t < t_b < 1$, it follows that ellipticity is first lost at $r = a$ and that this occurs when $t_a = 2 - \sqrt{3}$. For a given value of radius ratio $\alpha = b/a$, the corresponding value of the applied pressure, say p_e, is found from (3.17), where the value of t_b is given by (3.15) with $t_a = 2 - \sqrt{3}$. The corresponding value of $R(a)/a$ then follows from (3.21) with $p = p_e$ and $t_a = 2 - \sqrt{3}$. In Fig. 2, the pairs of values $(p_e/\mu, R(a)/a)$, for different radius ratios α, are joined by the dotted curve. There is a critical value of the radius ratio $\alpha = \alpha_c$ say, at which $p_e = p_m$. This may be found numerically from (3.17), (3.18), (3.19) with $t_a = 2 - \sqrt{3}$, and we find

$$\alpha_c \simeq 5.1. \tag{4.15}$$

Thus, for $\alpha < \alpha_c$, the load maximum is reached before loss of ellipticity occurs while for $\alpha > \alpha_c$, the converse is true.

In either case, after loss of ellipticity, the existence of the smooth solutions obtained

here is still ensured. In addition, the possibility exists that non-smooth deformation fields, with discontinuous deformation gradients and stresses, might occur. The argument provided in [1] shows that axisymmetric solutions with such discontinuities do not exist in the present problem. Weak solutions, if they exist, must necessarily be non-axisymmetric. There is also the possibility that surface bifurcations might occur, as in [1], but we shall not pursue this issue here.

5. THE PRESSURIZED HOLLOW SPHERE

In this section, we describe briefly how the foregoing considerations can be applied to the analogous problem of an internally pressurized hollow sphere.

5.1. *Formulation of problem*

We are concerned in what follows with the pressure loading of a sphere composed of the Blatz–Ko material. Let

$$D_0 = \{(r, \theta, \phi) \mid a < r < b, 0 < \theta \leqslant 2\pi, 0 \leqslant \phi \leqslant \pi\},$$

denote the hollow sphere in its undeformed configuration. The sphere is subjected to an internal pressure p.

The resulting deformation is a one-to-one mapping which takes the point with spherical polar coordinates (r, θ, ϕ) to the point (R, Θ, Φ) in the deformed region D. We assume that the deformation is an axisymmetric one so that

$$R = R(r) > 0, \quad \Theta = \theta \quad \text{and} \quad \Phi = \phi \quad \text{on} \quad D_0, \tag{5.1}$$

where $R(r)$ is to be determined.

The polar components of the deformation gradient tensor associated wth (5.1) are given by

$$\mathbf{F} = \operatorname{diag}(\dot{R}(r), R(r)/r, R(r)/r). \tag{5.2}$$

The principal stretches associated with the radial deformation (5.1) are

$$\lambda_r = \dot{R}(r), \quad \lambda_\theta = \lambda_\phi = R(r)/r. \tag{5.3}$$

The Blatz–Ko material is characterized in the three-dimensional case, by the elastic potential (see e.g. [7])

$$W(\lambda_1, \lambda_2, \lambda_3) = \mu/2(\lambda_1^{-2} + \lambda_2^{-2} + \lambda_3^{-2} + 2\lambda_2\lambda_2\lambda_3 - 5). \tag{5.4}$$

The principal components of true stress τ are given by

$$\begin{aligned} \tau_{ii} &= \frac{\lambda_i}{\lambda_1\lambda_2\lambda_3}\frac{\partial W}{\partial \lambda_i} \quad (\text{no sum on } i) \\ &= \mu(1 - J^{-1}\lambda_i^{-2}), \quad J = \lambda_1\lambda_2\lambda_3. \end{aligned} \tag{5.5}$$

Substitution from (5.3) and (5.4) into (5.5) yields

$$\tau_{RR}(r) = \mu\left(1 - \frac{r^2}{R^2\dot{R}^3}\right), \tag{5.6a}$$

$$\tau_{\Theta\Theta}(r) = \tau_{\Phi\Phi}(r) = \mu\left(1 - \frac{r^4}{\dot{R}R^4}\right). \tag{5.6b}$$

In the absence of body force, the equilibrium equations $\operatorname{div}\boldsymbol{\tau} = \mathbf{0}$ reduce to

$$\frac{\mathrm{d}}{\mathrm{d}r}\tau_{RR} + \frac{2\dot{R}}{R}(\tau_{RR} - \tau_{\theta\theta}) = 0, \quad \text{for } a < r < b, \tag{5.7}$$

which, by virtue of (5.6), yields the nonlinear second-order ordinary differential equation

$$3r^2R^3\ddot{R} - 2rR^3\dot{R} + 2r^4\dot{R}^4 = 0, \quad \text{for } a < r < b. \tag{5.8}$$

The prescribed (pressure) boundary conditions are

$$\tau_{RR} = -p \quad \text{at } r = a, \tag{5.9a}$$

$$\tau_{RR} = 0 \quad \text{at } r = b. \tag{5.9b}$$

5.2. *Solution of boundary-value problem*

Just as in the two-dimensional case, eqn (5.8) may be reduced to a first-order equation on making the substitution

$$t(r) = \frac{r\dot{R}(r)}{R(r)} > 0. \tag{5.10}$$

Equation (5.8) then yields

$$3r\dot{t}(r) - t(1-t)(2t^2+2t+5) = 0 \quad \text{for } a < r < b, \tag{5.11}$$

where $\dot{t} = \mathrm{d}t/\mathrm{d}r$. Again we assume that $t(r)$ is less than unity for $a < r < b$ and so deduce from (5.11) that

$$0 < t < 1, \quad \mathrm{d}t/\mathrm{d}r > 0 \quad \text{for } a < r < b. \tag{5.12}$$

Integration of (5.11) yields

$$r^{15} = \frac{Ct^9\mathrm{d}(t)}{(2t^2+2t+5)^2(1-t)^5}, \tag{5.13}$$

where C is a positive constant of integration and the function $\mathrm{d}(t)$ is defined by

$$\mathrm{d}(t) = \exp\left\{2\tan^{-1}\left(\frac{2t+1}{3}\right)\right\} > 0. \tag{5.14}$$

Also (5.10), (5.11) yield

$$R^6 = D\frac{(2t^2+2t+5)\mathrm{d}(t)}{(1-t)^2}, \tag{5.15}$$

where $D > 0$ is a constant of integration. The range of the parameter t is

$$(0 <)\, t_a < t < t_b\, (< 1). \tag{5.16}$$

The components of true stress τ_{RR}, $\tau_{\theta\theta}$ may also be expressed in terms of t on using (5.6), (5.10), (5.13) and (5.14). This leads to

$$\tau_{RR} = \mu\left\{1 - \left(\frac{C^2}{D^5}\right)^{1/6}(2t^2+2t+5)^{-3/2}\mathrm{d}^{-1/2}(t)\right\}, \tag{5.17}$$

$$\tau_{\Theta\Theta} = \mu\left\{1-\left(\frac{C^2}{D^5}\right)^{1/6} t^2(2t^2+2t+5)^{-3/2}\mathrm{d}^{-1/2}(t)\right\}, \tag{5.18}$$

for $t_a < t < t_b$.

From the definition of t_a and t_b, it follows from (5.13) that

$$a^{15} = \frac{Ct_a^9\mathrm{d}(t_a)}{(2t_a^2+2t_a+5)^2(1-t_a)^5}, \tag{5.19}$$

$$b^{15} = \frac{Ct_b^9\mathrm{d}(t_b)}{(2t_b^2+2t_b+5)^2(1-t_b)^5}. \tag{5.20}$$

Finally the boundary conditions (5.9), in view of (5.17), may be written as

$$-p = \mu\left\{1-\left(\frac{C^2}{D^5}\right)^{1/6}(2t_a^2+2t_a+5)^{-3/2}\mathrm{d}^{-1/2}(t_a)\right\}, \tag{5.21}$$

$$0 = \mu\left\{1-\left(\frac{C^2}{D^5}\right)^{1/6}(2t_b^2+2t_b+5)^{-3/2}\mathrm{d}^{-1/2}(t_b)\right\}. \tag{5.22}$$

The four equations (5.19)–(5.22) for the four unknowns t_a, t_b, C, D are analogous to eqns (3.11)–(3.14) obtained in the two-dimensional case. It can be verified that the considerations of sub-section 3.2 carry over, with obvious modification, to the three-dimensional equations of concern here. In particular, the analog of (3.21) in the present case is given by

$$\frac{R(a)}{a} = t_a^{-3/5}\left(1+\frac{p}{\mu}\right)^{-1/5} \tag{5.23}$$

5.3. *Thin shell*

When the radius ratio $\alpha(=b/a)$ is very near to unity, the explicit relation between t_a and prescribed pressure, analogous to (4.4), is given by

$$\frac{p}{\mu} = 2\varepsilon(t_a-t_a^3)+O(\varepsilon^2), \quad \varepsilon = \frac{b-a}{a} \ll 1. \tag{5.24}$$

Similarly, the analog of (4.5), on using (5.23), (5.24) becomes

$$\frac{R(a)}{a} = t_a^{-3/5}+O(\varepsilon). \tag{5.25}$$

A graph of the ratio of the deformed radius to undeformed radius vs pressure, according to (5.24) and (5.25), is shown in Fig. 3. Again we observe that the pressure first increases as the shell inflates, reaches a maximum with value $0.7698\mu\varepsilon$ where $R(a) = 1.390a$ and decreases on further inflation.

5.4. *Thick shell*

For a thick shell, numerical computation yields the graph of pressure vs deformed radius shown in Fig. 4. The behavior of the spherical shell is similar to that of the cylindrical shell shown in Fig. 2.

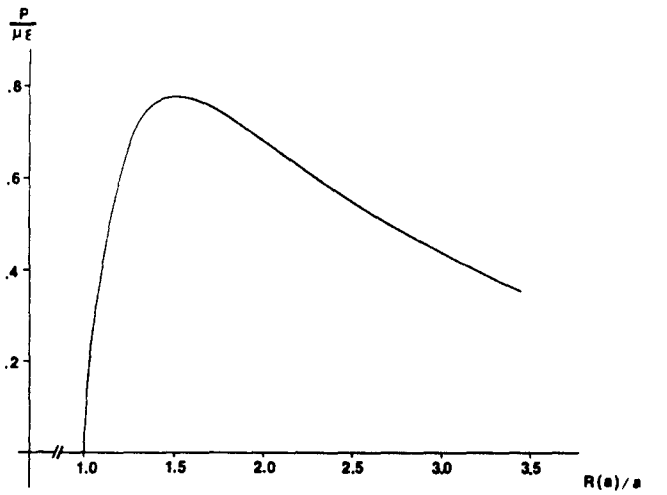

Fig. 3. Applied pressure vs ratio of deformed to undeformed radius for a thin spherical shell.

5.5. *Linearization*

For small pressure ($p/\mu \ll 1$), we find again that $t_a \simeq 1$, $t_b \simeq 1$ and so $t(r) \simeq 1$ throughout the body. Let

$$t_a = 1-\delta_a, \quad t_b = 1-\delta_b, \quad t(r) = 1-\delta(r) \tag{5.26}$$

where the small parameters δ_a, δ_b and $\delta(r)$ are unknown. We find that

$$\tau_{\theta\theta} = 2\mu/3(\delta+2\delta_b), \tag{5.27a}$$

$$\tau_{RR} = 4\mu/3(\delta_b-\delta), \tag{5.27b}$$

$$p/\mu = 4/3(\delta_a-\delta_b), \tag{5.27c}$$

$$\delta(r) = (a^3/r^3)\delta_a, \tag{5.27d}$$

$$\delta_b = \alpha^{-3}\delta_a, \quad \alpha = b/a. \tag{5.27e}$$

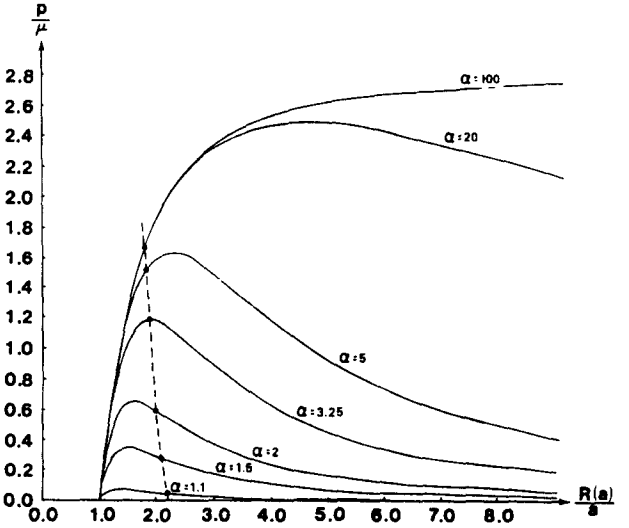

Fig. 4. Applied pressure vs ratio of deformed to undeformed radius for hollow spheres for different radius ratios $\alpha = b/a$. The dotted curve connects the points $(p_e/\mu, R(a)/a)$, where p_e denotes the pressure at which ellipticity is lost.

The resulting linearized stress fields given by (5.27) again yield the well-known results of the infinitesimal theory of elasticity (see e.g. Timoshenko and Goodier[11], p. 395),

$$\tau_{RR} = \frac{pa^3}{b^3-a^3}\left(1-\frac{b^3}{r^3}\right), \tag{5.28a}$$

$$\tau_{\Theta\Theta} = \frac{pa^3}{2(b^3-a^3)}\left(2+\frac{b^3}{r^3}\right). \tag{5.28b}$$

5.6. *Loss of ellipticity*

In the three-dimensional case also, for the Blatz–Ko material, necessary and sufficient conditions for ellipticity of the displacement equations of equilibrium have been obtained by Knowles and Sternberg[8]. Thus from eqn (3.1) of [8] it follows that ellipticity holds for the Blatz–Ko material (5.4) at the axisymmetric solution (5.1) if and only if the principal stretches λ_r, λ_θ, λ_ϕ introduced in (5.3) are such that

$$2-\sqrt{3} < \lambda_r/\lambda_\theta < 2+\sqrt{3}, \tag{5.29a}$$

$$2-\sqrt{3} < \lambda_r/\lambda_\phi < 2+\sqrt{3}, \tag{5.29b}$$

$$2-\sqrt{3} < \lambda_\phi/\lambda_\theta < 2+\sqrt{3}. \tag{5.29c}$$

Since in this problem we have $\lambda_\theta = \lambda_\phi$, (5.29c) is automatically satisfied and (5.29a), (5.29b) are equivalent to

$$2-\sqrt{3} < t < 2+\sqrt{3}, \quad t = \lambda_r/\lambda_\theta = \lambda_r/\lambda_\phi. \tag{5.30}$$

The inequality on the right in (5.30) always holds (see (5.12)) and, by virtue of the monotone increasing character of t as r increases (see (5.12)), ellipticity is first lost at $r = a$ and this occurs when $t_a = 2-\sqrt{3}$. For a given value of the radius ratio $\alpha = b/a$, the corresponding value of the applied pressure, say p_e, is found in a similar manner to the two-dimensional case on using (5.19)–(5.22). The corresponding value of $R(a)/a$ then follows from (5.23) with $p = p_e$ and $t_a = 2-\sqrt{3}$. In Fig. 4, the pairs of values $(p_e/\mu, R(a)/a)$ for different radius ratios α are joined by the dotted curve. As in the case of the two-dimensional problem, there is a critical value of the radius ratio $\alpha = \alpha_c$ at which $p_e = p_m$. This may be found numerically and we find that

$$\alpha_c \simeq 3.25.$$

Thus for $\alpha < \alpha_c$, the pressure maximum is reached before loss of ellipticity while for $\alpha > \alpha_c$, the converse is true. Finally, after loss of ellipticity, the non-existence of non-smooth axisymmetric solutions may be demonstrated by an obvious modification of the argument given in [1]. The possibility of surface bifurcations also exists, but we shall not pursue this here.

Acknowledgements—This work was supported by the U.S. Army Research Office under Grant DAAG 29-83-K-0145 (C. O. Horgan and R. Abeyaratne) and by the U.S. National Science Foundation under Grants MEA 78-26071 and MSM 85-12825 (C.O.H.) and MEA 83-19616 (R.A.). This research is part of a dissertation[10] submitted in partial fulfillment of the requirements for the Ph.D. degree at Michigan State University.

REFERENCES

1. R. Abeyaratne and C. O. Horgan, Initiation of localized plane deformations at a circular cavity in an infinite compressible nonlinearly elastic medium. *J. Elasticity* **15**, 243–256 (1985).
2. A. E. Green and W. Zerna, *Theoretical Elasticity*. Oxford University Press, Oxford (1968).
3. R. W. Ogden, *Non-Linear Elastic Deformations*. Halsted Press, New York (1984).
4. R. Abeyaratne and C. O. Horgan, The pressurized hollow sphere problem in finite elastostatics for a class of compressible materials. *Int. J. Solids Structures* **20**, 715–723 (1984).

5. A. H. Jafari, R. Abeyaratne and C. O. Horgan, The finite deformation of a pressurized circular tube for a class of compressible materials. *J. appl. Math. Phys.* (*ZAMP*) **35**, 227–246 (1984).
6. R. W. Ogden and D. A. Isherwood, Solution of some finite plane strain problems for compressible elastic solids. *Q. J. Mech. appl. Math.* **31**, 219–249 (1978).
7. P. D. Blatz and W. L. Ko, Application of finite elasticity to the deformation of rubbery materials. *Trans. Soc. Rheol.* **6**, 223–251 (1962).
8. J. K. Knowles and E. Sternberg, On the ellipticity of the equations of nonlinear elastostatics for a special material. *J. Elasticity* **5**, 341–361 (1975).
9. M. M. Carroll, Load maxima for inflation of incompressible elastic hollow spheres and cylinders, *Q. appl. Math.* (1986), in press.
10. D.-T. Chung, The deformation and stability of a pressurized circular tube and spherical shell in finite elasticity and finite plasticity. Ph.D. dissertation, Michigan State University (1986).
11. S. P. Timoshenko and J. N. Goodier, *Theory of Elasticity*, 3rd edn. McGraw-Hill, New York (1970).